**Targeting autophagy to modulate cell survival: a comparative analysis in cancer, normal and embryonic cells**

Aleksandra Divac Rankov[1], Mila Ljujić[1], Marija Petrić[1], Dragica Radojković[1], Milica Pešić[2], Jelena Dinić[2*]

[1]Institute of Molecular Genetics and Genetic Engineering, University of Belgrade, Belgrade, Serbia

[2]Institute for Biological Research, Department of Neurobiology, University of Belgrade, Belgrade, Serbia

[*]Corresponding author

Jelena Dinić, PhD

Institute for Biological Research, Department of Neurobiology, University of Belgrade, Despota Stefana 142, 11 060 Belgrade, Serbia

Phone: +381 11 20 78 406

Fax: +381 11 27 61 433

Email: jelena.dinic@ibiss.bg.ac.rs

**Acknowledgements**

This research was supported by Ministry of Education, Science and Technological Development of Serbia (grant nos. III41031 and 173008).

**Abstract**

Autophagy is linked to multiple cancer-related signaling pathways, and represents a defense mechanism for cancer cells under therapeutic stress. The crosstalk between apoptosis and autophagy is essential for both tumorigenesis and embryonic development. We studied the influence of autophagy on cell survival in pro-apoptotic conditions induced by anticancer drugs in three model systems: human cancer cells (NCI-H460, COR-L23 and U87), human normal cells (HaCaT and MRC-5) and zebrafish embryos (*Danio rerio*).

Autophagy induction with AZD2014 and tamoxifen antagonized the pro-apoptotic effect of chemotherapeutics doxorubicin and cisplatin in cell lines, while autophagy inhibition by wortmannin and chloroquine synergized the action of both anticancer agents. This effect was further verified by assessing cleaved caspase 3 and PARP-1 levels. Autophagy inhibitors significantly increased both apoptotic markers when applied in combination with doxorubicin while autophagy inducers had the opposite effect. In a similar manner, autophagy induction in zebrafish embryos prevented cisplatin-induced apoptosis in the tail region while autophagy inhibition increased cell death in the tail and retina of cisplatin-treated animals. Autophagy modulation with direct inhibitors of the PI3kinase/Akt/mTOR pathway (AZD2014 and wortmannin) triggered the cellular response to anticancer drugs more effectively in NCI-H460 and zebrafish embryonic models compared to HaCaT suggesting that these modulators are selective towards rapidly proliferating cells. Therefore, evaluating the autophagic properties of chemotherapeutics could help determine more accurately the fate of different cell types under treatment. Our study underlines the importance of testing autophagic activity of potential anticancer agents in a comparative approach to develop more rational anticancer therapeutic strategies.

**Keywords:** autophagy, apoptosis, caspase-3, PARP-1, cancer cells, zebrafish

## Introduction

Autophagy is an evolutionary conserved mechanism characterized by degradation and recycling of cellular components. Ubiquitinated components are sequestered into autophagic vesicles and subsequently degraded through fusion with lysosomes (Eskelinen and Saftig 2009). Autophagy has a dual role in cellular homeostasis, promoting both cell survival and cell death (Aredia et al. 2012). Although autophagy occurs at a basal level in mammalian cells, it is often upregulated in response to a range of both physiological and non-physiological conditions.

In cancer cells, autophagy is triggered in response to cellular stress, such as nutrient and growth factor starvation, or hypoxia and can act as either tumor suppressor or tumor promoter (Mathew et al. 2007). Such diverse role of autophagy largely depends on the type and genetic background of cancer cells (Janji et al. 2013). Although autophagy is linked to multiple cancer-related pathways, the most relevant and best studied is phosphatidylinositol 3-kinase/protein kinase B/mammalian target of rapamycin (PI3kinase/Akt/mTOR) signaling pathway (Meijer and Codogno 2004). Multiple studies demonstrated that tumor cells can survive anticancer treatment upon activating autophagy (Mathew et al. 2007; Hippert et al. 2006; Janji et al. 2013). Furthermore, autophagy can act as a resistance mechanism of cancer cells under therapeutic stress and prevent cell death by blocking apoptosis (Martinet et al. 2009). Therefore, autophagy has an important role in developing cancer multidrug resistance.

Autophagy is also associated with tissue remodeling essential for the development of vertebrates (Aburto et al. 2012). During embryonic development, activation of the autophagic machinery can promote cell death, proliferation or differentiation under different conditions. In recent years, zebrafish (*Danio rerio*) emerged as a useful vertebrate model system for investigating the mechanisms behind these processes. Interplay between autophagy and apoptosis was shown to be an important part of both development and injury-induced tissue renewal in zebrafish (Cole and Ross 2001; Lee et al. 2014; Varga et al. 2014). Research has shown that genetic and pharmacological inhibition of autophagy impaired the regeneration of amputated caudal fins in the zebrafish and upregulation of autophagy in the regeneration zone protected cells from undergoing apoptosis (Varga et al. 2014). Using GFP-LC3 expressing zebrafish, Lee and coworkers found that during the embryonic period autophagy activates early on and in multiple tissues. Analysis of the temporal expression pattern detected RNA transcripts of autophagy-related genes from 1-cell stage embryos up to 48 hours post fertilization (hpf) (Lee et al. 2014).

Apoptosis, as a programmed cell death, plays a fundamental role in embryonic development and tissue homeostasis. Defects in this process can lead to various diseases, including cancer and neurodegenerative disorders (Thompson 1995). The apoptotic mechanisms in zebrafish are very similar to those in mammals with significant amount of homology in apoptosis-related genes including Bcl-2 family members, caspases, apoptosis-related kinases and transcriptional factors, implying high degree of preservation in cell death pathways within vertebrates (Inohara and Nunez 2000). There is a normal apoptosis pattern during zebrafish development and apoptotic cells can regularly be observed in various tissues and organs (Cole and Ross 2001; Detrich et al. 2010).

Apoptosis and autophagy are in a complex crosstalk sharing molecular components that directly regulate them and can be triggered by common upstream signals (Fimia and Piacentini 2010). Both processes can either induce cell death in a coordinated fashion, or the cell can switch between the two responses in a mutually exclusive manner. Consequently, autophagy can antagonize apoptotic cell death by promoting cell survival, and apoptosis-associated caspase activation can disrupt the autophagic process.

Understanding the interplay between these key processes in cancer and other diseases is fundamental for the development of successful therapy. When autophagy is manipulated for therapeutic purposes, it is crucial to recognize its role in both cytoprotection and cytotoxicity, since interfering with one type of cell death may activate another cell-damaging pathway. Considering the evolutionary conservation of autophagic and apoptotic mechanisms, comparative studies of the zebrafish embryos and human cells can provide novel insights on the two processes, understand their role in human disease and help develop new treatments based on autophagy modulation.

In this study, we investigated the influence of autophagy on cell survival in pro-apoptotic conditions induced by anticancer drugs in cancer, normal and embryonic cells. Autophagy was inhibited with wortmannin or chloroquine while AZD2014 or tamoxifen served as autophagy inducers. We employed five human cell lines, NCI-H460 and COR-L23 non-small cell lung carcinoma and U87 glioblastoma as a model for cancer cells while HaCaT keratinocytes and MRC-5 embryonic lung fibroblasts served as a model for normal cells. For further evaluation, zebrafish embryos were engaged as *in vivo* model system for embryonic cells. Our results demonstrated the similarities and differences regarding autophagy as a cellular survival response in the three aforementioned models.

## Materials and Methods

### Drugs

Doxorubicin (DOX) solution was obtained from EBEWE Arzneimittel GmbH (Vienna, Austria). Cisplatin (CPt) was obtained from Pfizer (Perth) Pty Ltd (Bentley, Australia). AZD2014 and wortmannin (WORT) were kindly provided by SelleckChem (Houston, TX, USA). Tamoxifen (TMX) and chloroquine (CQ) were purchased from Sigma-Aldrich Chemie GmbH (Munich, Germany).

### Reagents

RPMI 1640 medium, DMEM medium, penicillin–streptomycin solution, antibiotic–antimycotic solution, L-glutamine and trypsin/EDTA were purchased from PAA (Vienna, Austria). Fetal bovine serum (FBS), dimethyl sulfoxide (DMSO) and Thiazolyl blue tetrazolium bromide (MTT) were obtained from Sigma-Aldrich Chemie GmbH. Acridine orange was purchased from Alfa Aesar (Heysham, UK) and Hoechst 33342 was from Thermo Fisher Scientific (Waltham, USA). Annexin-V-FITC (AV) and propidium iodide (PI) were purchased from Abcam (Cambridge, UK). Bovine serum albumin (BSA) was from Serva (Heidelberg, Germany) and Triton™ X-100 was obtained from Merck KGaA (Darmstadt, Germany). Rabbit anti- microtubule-associated protein-1 light chain 3 (LC3) and rabbit anti-Phospho-Akt (Ser473) Alexa Fluor 647 conjugated (pAkt) antibodies were purchased from Cell Signaling Technology® (MA, USA). Goat anti-cleaved caspase-3 and mouse anti-cleaved Poly(ADP-ribose) polymerase-1 (PARP-1) antibodies were from Santa Cruz Biotechnology (CA, USA). Rabbit anti-p62/SQSTM1 antibody was obtained from Novus Biologicals (MN, USA). Secondary antibodies Alexa Fluor 488 goat anti-Rabbit IgG(H+L), Alexa Fluor 555 goat anti-Rabbit IgG(H+L), Alexa Fluor 488 goat anti-Mouse IgG(H+L), and Alexa Fluor 488 donkey anti-Goat IgG(H+L) were purchased from Thermo Fisher Scientific (Waltham, USA). Tricaine-S was obtained from Western Chemicals Inc (WA, USA).

### Cell culture

Human non-small cell lung carcinoma (NSCLC) cells NCI-H460, normal human embryonic lung fibroblasts MRC-5 and human glioblastoma U87 cell line were purchased from the American Type Culture Collection (ATCC, Rockville, MD, USA). Another human NSCLC-derived cell line, COR-L23 was purchased from the European Collection of Cell

Cultures (ECACC, Salisbury, UK). NCI-H460 and COR-L23 cells were maintained in RPMI 1640 supplemented with 10% FBS, 2 mM L-glutamine, 4.5 g/L glucose, 10,000 U/mL penicillin, 10 mg/mL streptomycin, 25 mg/mL amphotericin B solution. U87 cells were cultured in MEM supplemented with 10% FBS, L-glutamine (2 mM) and 5000 U/mL penicillin, 5 mg/mL streptomycin solution. HaCaT cell line (obtained from CLS - Cell Lines Service) was generous gift from Prof. Jörg Andrä, Division of Biophysics, Research Center Borstel, Leibniz-Center for Medicine and Biosciences, Borstel, Germany. HaCaT and MRC-5 cells were cultured in DMEM supplemented with 10% FBS, 4 g/L glucose, L-glutamine (2 mM) and 5,000 U/mL penicilin, 5 mg/mL streptomycin solution. All cell lines were subcultured at 72 h intervals using 0.25% trypsin/EDTA and seeded into a fresh medium at the following densities: 8,000 cells/$cm^2$ for NCI-H460, COR-L23 and MRC-5 cells, and 16,000 cells/$cm^2$ for U87 and HaCaT cells. All cell lines were maintained at 37 °C in a humidified 5% $CO_2$ atmosphere.

**Cytotoxicity by MTT assay**

Cell viability was assessed by MTT assay according to the manufacturer's instructions. Briefly, cells were seeded overnight in 96-well tissue culture plates (1,000 cells/well for NCI-H460 and COR-L23; 2,000 cells/well for HaCaT and MRC-5; 4,000 cells/well for U87) and then treated with increasing concentrations of DOX or CPt for 72 h (Table 1). In addition, NCI-H460, COR-L23, U87, HaCaT and MRC-5 cells were treated with increasing concentrations of WORT, CQ, AZD2014 or TMX (Table 1).

The combined effects of WORT, CQ, AZD2014 or TMX with DOX or CPt after 72 h were also studied. In co-treatments, 5 μM WORT, 20 μM CQ, 100 nM AZD2014 or 2.5 μM TMX, were combined with increasing concentrations of DOX (10 nM, 25 nM and 50 nM) or CPt (0.5 μM, 1 μM and 2.5 μM) and cells were grown at 37 °C for 72 h. Finally, MTT solution (1 mg/mL) was added to each well and plates were incubated at 37°C for 4 h. The absorbance was measured at 540 nm by an automatic microplate reader (LKB 5060-006 Micro Plate Reader, Vienna, Austria). $IC_{50}$ was calculated by linear regression analysis in Excel software.

**Median effect analysis**

The nature of interaction between inhibitors (WORT, CQ, AZD2014 or TMX) and DOX or CPt was analyzed using CalcuSyn software (Biosoft) that uses the combination index (CI) method (Chou and Talalay 1984), based on the multiple drug effect equation. At least three

data points were used for each single drug in each designed experiment. The non-constant ratio combination was chosen to assess the effect of both drugs in combination. The results are presented by fraction-affected CI graphs. Values of CI < 1 point to a pronounced additive effect or synergism, that is, the smaller value, the greater the degree of synergy. A value of CI = 1 indicates an additive effect, and values of CI > 1 point to an antagonistic effect.

**Cell death detection by flow cytometry**

The percentages of apoptotic, necrotic and viable cells were determined by Annexin-V-FITC and propidium iodide labeling according to the manufacturer's instructions. NCI-H460, COR-L23, HaCaT and MRC-5 cells were seeded and incubated overnight in 6-well plates at density of 100,000 cells/well. NCI-H460 and HaCaT cells were treated for 72 h with 5 μM WORT, 20 μM CQ, 100 nM AZD2014 and 2.5 μM TMX as well as their combinations with 20 nM DOX. COR-L23 cells were treated with 5 μM WORT, 20 μM CQ, 100 nM AZD2014 and 2.5 μM TMX and their combinations with 80 nM DOX, while MRC-5 cells were treated with 5 μM WORT, 10 μM CQ, 100 nM AZD2014 and 2.5 μM TMX and their combinations with 80 nM DOX. The attached and floating cells were collected by centrifugation and AV/PI staining of the cells was analyzed within 1 h by flow cytometry. The fluorescence intensity was measured in green FL1-H and red FL2-H channel on CyFlow Space flow cytometer (Partec, Münster, Germany). In each sample, 10,000 cells were recorded, and the percentages of viable (AV− PI−), early apoptotic (AV+ PI−), late apoptotic (AV+ PI+), and necrotic (AV− PI+) cells were analyzed by Summit analysis software (Dako Colorado Inc., USA).

**Detection of cleaved capase-3, PARP-1, p62 and pAkt levels by flow cytometry**

The protein levels of apoptosis markers were detected on a flow cytometer by measuring the fluorescence intensity of anti-cleaved caspase-3 antibody coupled with secondary Alexa Fluor 488 donkey anti-Goat IgG(H+L) antibody, and anti-cleaved PARP-1 antibody coupled with secondary Alexa Fluor 488 goat anti-Mouse IgG(H+L) antibody. The protein levels of p62 and phosphorylated Akt were detected by measuring the fluorescence intensity of anti-p62 antibody coupled with secondary Alexa Fluor 488 goat anti-Rabbit IgG(H+L) antibody, and anti-pAkt antibody conjugated with Alexa Fluor 647. NCI-H460, COR-L23, HaCaT and MRC-5 cells were grown overnight in 6-well plates (seeding density 100,000 cells/well), and then treated for 72 h at 37 °C. NCI-H460 and HaCaT were treated with 5 μM WORT, 20 μM CQ, 100 nM AZD2014 or 2.5 μM TMX as well as their combinations with 20 nM DOX. COR-L23 cells were treated with 5 μM WORT, 20 μM CQ, 100 nM AZD2014 and 2.5 μM

TMX and their combinations with 80 nM DOX, while MRC-5 cells were treated with 5 μM WORT, 10 μM CQ, 100 nM AZD2014 and 2.5 μM TMX and their combinations with 80 nM DOX. Adherent cells were harvested by trypsinization, washed twice in PBS and fixed in 4% paraformaldehyde for 10 min at room temperature. NCI-H460, COR-L23, HaCaT and MRC-5 cells were then permeabilized by adding ice-cold 90% methanol and stored at −20 °C overnight. After washing in PBS, cells were blocked for 1 h with 0.5% BSA in PBS. Cells were then resuspended in primary antibody diluted in 0.5% BSA (1:1000) and incubated 1 h at room temperature. After washing in PBS, cells labeled with unconjugated primary antibody were resuspended in secondary antibody diluted in 0.5% BSA (1:1000) and incubated for 30 min at room temperature. NCI-H460, COR-L23, HaCaT and MRC-5 cells were subsequently washed and resuspended in 500 μL of PBS. The fluorescence intensity was measured in FL1-H or FL3-H channel on CyFlow Space flow cytometer and analyzed by Summit analysis software.

**Cell lines immunohistochemistry and fluorescence microscopy**

NCI-H460, COR-L23, HaCaT and MRC-5 cells were seeded in 8-well chamber-slides (Labtek, Nunc, USA) and allowed to grow at 37°C overnight before treatment. Then, NCI-H460 and HaCaT were treated for 72 h with 5 μM WORT, 20 μM CQ, 100 nM AZD2014 or 2.5 μM TMX as well as their combinations with 20 nM DOX. COR-L23 cells were treated with 5 μM WORT, 20 μM CQ, 100 nM AZD2014 and 2.5 μM TMX and their combinations with 80 nM DOX, while MRC-5 cells were treated with 5 μM WORT, 10 μM CQ, 100 nM AZD2014 and 2.5 μM TMX and their combinations with 80 nM DOX. Cells were fixed in 4% paraformaldehyde, blocked for 1 h with 2% BSA/0.3% Triton™ X-100 in PBS and then incubated with primary antibodies in 0.5% BSA in PBS overnight at 4°C. LC3 is one of the main markers of autophagy involved in the autophagosome formation (Tanida et al. 2005). To detect autophagosomes, anti-LC3 antibody was applied at 1:500 dilution. Polyubiquitin-binding protein p62 is another common autophagy marker whose total cellular expression levels inversely correlate with autophagic activity (Mizushima et al. 2010). To detect p62 levels, anti-p62 antibody was applied at 1:1000 dilution. To detect p17 subunit of cleaved caspase-3 and examine the cellular localization of cleaved PARP-1, anti-caspase-3 and anti-cleaved PARP-1 antibodies were applied at 1:1000 dilution and cells were incubated overnight at 4°C. After washing in PBS, corresponding secondary antibodies (anti-rabbit Alexa Fluor 488, anti-rabbit Alexa Fluor 555, anti-goat Alexa Fluor 488 or anti-mouse Alexa Fluor 488) were applied at 1:1000 dilution in 0.5% BSA in PBS in dark for 2 h at room

temperature. Nuclei were counterstained with Hoechst 33342 for 15 min at room temperature and cells were mounted in Mowiol (Sigma-Aldrich Chemie GmbH). NCI-H460, COR-L23, HaCaT and MRC-5 cells were visualized under the Zeiss Axiovert inverted fluorescent microscope (Carl Zeiss Foundation, Oberkochen, Germany) equipped with AxioVision4.8 software.

**Zebrafish stocks and maintenance**

Zebrafish, Tübingen wild type strain, were maintained at 28 °C in 14:10 h light/dark cycle and fed twice daily with flake food and once daily with live brine shrimp. Zebrafish embryos were collected from pairwise mating of adults and kept and handled in egg water containing 0.073 mM KCl, 2 mM $CaCl_2$, 0.5 mM MgSO4, and 0.0002% methylene blue with the addition of sodium bicarbonate to final concentration of 0.75 mM. Maintenance, embryo collection, staging and incubation were conducted according to standard procedures and guidelines (Westerfield 2000). All animal handling was in accordance with local and national regulations.

**Zebrafish drug treatment**

At 6 hpf embryos were transferred into 24-well plates (12 embryos per well) and treated with selected autophagy modulators at non-toxic concentrations (2.5 μM WORT, 250 μM CQ, 100 nM AZD2014, 2.5 μM TMX) or with the combinations of these compounds with 250 μM CPt. As DOX treatment of zebrafish embryos did not produce substantial cell death in selected experimental conditions, CPt was used to induce apoptosis in this model. Autophagy modulator concentrations with at least 90% embryo survival rate were considered non-toxic and selected for further treatments. The embryo survival was monitored at 24 hpf and 48 hpf. At 48 hpf the remaining chorions were manually removed and embryos were anesthetized in a 1:10 dilution of 0.003% Tricaine-S. Each experiment was carried out in triplicates and repeated at least three times.

**Acridine orange apoptosis assay**

Acridine orange is a vital DNA intercalating dye used to visualize the nuclei in apoptotic cells (Brand et al. 1996). Dechorionated live embryos were incubated in 10μg/mL acridine orange at 28°C for 30 min and washed 3 times in water. Anesthetized embryos were then mounted in water containing Tricaine-S (0.003%) and imaged in a 3.5-cm glass-bottom culture dish on Leica TSC SP8 confocal microscope using 10x/0.3 NA lens. All confocal

images were processed using ImageJ software (U.S. National Institutes of Health, Bethesda, MD, USA) and represent maximum projections of z-stacks.

**Zebrafish immunohistochemistry and confocal microscopy**

For whole-mount immunostaining, deyolked embryos were fixed in 4% paraformaldehide overnight and then kept in methanol at −20 °C until staining. Embryos were rehydrated by sequential washing with gradient dilution of methanol and then permeabilized with 0.2% Triton™ X-100 in PBS (PBST) by heating at 70 °C for 15 min and blocked with 2% BSA in PBST for 2 h at room temperature. Embryos were then incubated with primary antibodies (anti-LC3, anti-p62, anti-cleaved caspase-3 or anti-cleaved PARP-1) in PBST overnight at 4 ˚C. Embryos were then washed in PBST 4 times and incubated with corresponding secondary antibodies (anti-rabbit Alexa Fluor 488, anti-rabbit Alexa Fluor 555, anti-goat Alexa Fluor 488 or anti-mouse Alexa Fluor 488) at 1:1000 dilution in PBST in dark, overnight at 4 ˚C. Hoechst 33342 was added 2 h before the end of the incubation and samples were kept in dark at 37 ˚C with constant mixing. Stained embryos were mounted in glycerol and imaged on Leica TSC SP8 confocal microscope (Leica Microsystems) using 63/1.4 NA oil immersion lens.

**Statistical analysis**

Statistical analysis for flow-cytometric data was performed by two-way ANOVA test (GraphPad Prism software) and the differences between groups were determined by Dunnett's multiple comparisons test. Statistical significance was accepted if $p < 0.05$.

**Results**

**Sensitivity of cancer and normal cells to anticancer drugs after autophagy modulation**

The growth inhibition effect of autophagy inhibitors (WORT and CQ) and inducers (AZD2014 and TMX) on NCI-H460, COR-L23, U87, HaCaT and MRC-5 cells were evaluated by MTT cytotoxicity assay. The cytotoxicity of two classic chemotherapeutics and potent pro-apoptotic agents DOX and CPt was also evaluated in all cell lines. The results obtained after the 72 h treatment are shown in Fig. 1a and Online Resource Fig. S1.

The $IC_{50}$ values of DOX and CPt in single and combined treatments with autophagy modulators are summarized in Table 2. The $IC_{50}$ values of autophagy modulators are also presented. DOX was not selective towards cancer cells in this experimental system and

among all tested cell lines the lowest $IC_{50}$ values were obtained in NCI-H460 and HaCaT cells (41.7 nM and 29.2 nM, respectively). CPt also exerted non-selective inhibitory effect in tested cell lines (Table 2, Fig. 1b). Between autophagy inhibitors, WORT was most active in NCI-H460 and HaCaT cells, while CQ showed significantly higher efficacy in both normal cell lines compared to cancer cells (Table 2). Between autophagy inducers, AZD2014 was most active in NCI-H460 among cancer cell lines and selective towards NCI-H460 cells with 3 fold lower $IC_{50}$ value when compared to HaCaT and 10 fold lower $IC_{50}$ value compared to MRC-5 cells. TMX was most efficient in U87 and MRC-5 cells with $IC_{50}$ values ranging from approximately 5 to 15 μM in tested cell lines.

Concentrations of autophagy modulators that displayed moderate to low cell growth inhibition in tested cell lines were chosen for autophagy modulation in further experiments and for combination treatments.

The nature of interaction between autophagy modulators with DOX and CPt was investigated during combined treatments. Autophagy inhibitors WORT and CQ increased the sensitivity of cancer and normal cell lines to classic chemotherapeutics. On contrary, autophagy inducers AZD2014 and TMX significantly decreased the chemosensitivity of tested cell lines (Fig. 1b, Table 2). The chemosensitization with CQ was not observed only in U87 cells. Analysis of the nature of interaction between the two drugs revealed that WORT and CQ combinations with DOX have a pronounced synergistic effect (CI < 1). AZD2014 and TMX combinations with DOX resulted in a prominent antagonism (CI > 1), especially in NCI-H460 cells (Fig. 1c). Combined treatments of each autophagy modulator with CPt displayed a similar, although less notable effect in NCI-H460 and HaCaT cells (Fig. 1c). Comparable trend was detected in COR-L23 and MRC-5 cells, although the synergistic effect with WORT was observed at lower CPt concentrations in COR-L23, while in MRC-5 cell line antagonism with AZD2014 was present at higher DOX concentrations (Online Resource Fig. S2). In U87 cells, synergistic effect was detected only with WORT in both DOX and CPt co-treatments, while combinations with CQ were dose-dependent and synergism was observed only at higher CPt concentrations and was not present with DOX. The synergistic/antagonistic interaction of autophagy inhibitors/inducers with chemotherapeutics was the most evident in NCI-H460 among cancer cell lines while HaCaT as a normal cells model showed higher sensitivity to most tested compounds and these cell lines were selected for the majority of further studies. Since combinations with DOX had a more prominent antagonistic or synergistic effect on the modulation of the cell survival, concentration

approximate to $IC_{30}$ value for DOX in NCI-H460 cells was chosen for further experiments on selected cell lines.

**Autophagy modulation in cancer and normal cells**

To confirm that autophagy modulators interfered with autophagy in cancer and normal cells at selected concentrations, we studied the cellular distribution of autophagosomal marker LC3 and autophagy flux marker p62.

Autophagic vesicles labeled with anti-LC3 antibody were visualized in NCI-H460 and HaCaT cells after 72 h treatment with WORT, CQ, AZD2014 or TMX as well as their combinations with DOX. Treatment with WORT, which inhibits phagophore formation, prevented the appearance of autophagic vesicles in NCI-H460 and HaCaT cells (Fig. 2a). Treatment with CQ, which inhibits autophagy by preventing the autophagosome/lysosome fusion, caused excessive cytoplasmatic accumulation of LC3 puncta. AZD2014 and TMX activated the autophagy process which resulted in the appearance of autophagosomes in the cytoplasm. Autophagy inhibitors WORT and CQ both prevented autophagy-mediated degradation of p62 causing its cytoplasmatic accumulation (Fig. 2b). The flow-cytometric profiles and quantification of p62 accumulation are presented in Online Resource Fig. S3. The presence of DOX in co-treatments did not interfere with the autophagy-modulating properties of the selected compounds. In COR-L23 and MRC-5 cell lines, which displayed a comparable trend to NCI-H460 and HaCaT regarding antagonistic or synergistic effects of DOX co-treatment, autophagy modulators interfered with autophagy in a similar manner. The flow-cytometric profiles and quantification of p62 accumulation as well as fluorescent microscopic images of LC3 and p62 labeling in COR-L23 and MRC-5 cells are presented in Online Resource Fig. S4.

**The effect of autophagy modulation on DOX-induced cell death in cancer and normal cells**

The impact of autophagy modulation on DOX-induced cell death was studied in cancer and normal cells treated for 72 h with DOX alone and in combination with WORT, CQ, AZD2014 or TMX. Cells were subsequently subjected to Annexin-V-FITC/Propidium Iodide staining and examined on a flow cytometer. Quantification and statistical analysis of the results obtained in NCI-H460 and HaCaT cells by flow cytometry is shown in Fig. 3a. The flow-cytometric profiles for each experimental condition are shown in Fig. 3b.

The addition of WORT did not significantly increase the amount of late apoptotic NCI-H460 cells. WORT caused a very small increase in early apoptotic and necrotic cells (from 1% to 4% and from 10% to 12%, respectively) and reduced the number of viable cells only from 79% to 74%. However, co-treatment with CQ significantly amplified the pro-apoptotic effect of DOX, decreasing the number of viable cells from 79% to 68% compared to a single DOX treatment. The percentage of cells in late apoptosis increased from 10% to 22%. The induction of autophagy with AZD2014 and TMX had the opposite effect on cell viability. Combination treatment with AZD2014 significantly reduced the percentage of late apoptotic and necrotic cells observed when DOX was applied alone (from 10% to 6% and from 10% to 4%, respectively). The percentage of viable cells increased from 79% to 90% in the same experimental conditions. Co-treatment with TMX produced a similar effect significantly increasing the percentage of viable NCI-H460 cells (from 79% to 89%) compared to cells treated only with DOX. TMX presence also significantly decreased the percentage of late apoptotic and necrotic cells (from 10% to 5% in both cases) compared to treatment with DOX alone.

Autophagy inhibition in normal keratinocytes showed a stronger synergy on DOX-induced apoptosis compared to NCI-H460 cells (Fig. 3a and 3b). WORT combination with DOX reduced viable cell number from 78% to 64% compared to a single DOX treatment, while late apoptotic and necrotic cells number rose from 6% to 13% and from 15% to 22%, respectively. Co-treatment with CQ considerably decreased the viable cells percentage from 78% to 35% compared to a single DOX treatment. Late apoptotic and necrotic cells percentages increased from 6% to 25% and from 15% to 41%, respectively. Comparable trend of autophagy inducers antagonizing pro-apoptotic activity of DOX was also observed in HaCaT cells.

In COR-L23 and MRC-5 cell lines autophagy modulators interfered with DOX-induced cell death in a similar manner. Quantification, statistical analysis and the flow-cytometric profiles for each experimental condition are presented in Online Resource Fig. S5. The percentage of late apoptotic and necrotic cells in both COR-L23 and MRC-5 cell lines after WORT or CQ co-treatment with DOX substantially increased compared to DOX treatment alone. AZD2014 combined with DOX significantly decreased the percentage of late apoptotic and necrotic (COR-L23) or late apoptotic cells (MRC-5) compared to single DOX treatment. Co-treatment with TMX produced a similar effect and antagonized DOX-induced cell death reducing the amount of late apoptotic and necrotic cells in both cell lines.

**The effect of autophagy modulation on cleaved caspase-3 and PARP-1 levels in cancer and normal cells**

To further investigate the impact of autophagy modulation on the apoptosis process, we assessed the cellular content of cleaved caspase-3 and PARP-1. Quantification and statistical analysis of flow-cytometric measurements of cleaved caspase-3 and PARP-1 levels is shown in Fig. 4a, while flow-cytometric profiles for each experimental condition are shown in Fig. 4b.

WORT in combination with DOX significantly raised only cleaved PARP-1 content in NCI-H460 cells compared to a single DOX treatment while co-treatment with CQ additionally elevated cellular levels of both apoptotic markers. Compared to single DOX treatment, overall cleaved caspase-3 and PARP-1 content in cancer cells was significantly lower after AZD2014 or TMX co-treatment. WORT and CQ co-treatment with DOX in HaCaT cells elevated cellular pool of both apoptotic markers compared to application of DOX alone. Additionally, CQ elevated pAkt levels in both cell lines and this was also observed in DOX co-treatment in HaCaT cells, while other autophagy modulators decreased pAkt content in NCI-H460 cells (Online Resource Fig. S3). AZD2014 combination with DOX significantly decreased only cleaved caspase-3 levels while combination with TMX decreased the total amount of cleaved caspase-3 and PARP-1 proteins in HaCaT cells.

In addition to flow-cytometric quantification, overall cellular content and localization of cleaved caspase-3 and PARP-1 proteins was visualized by fluorescent microscopy in NCI-H460 and HaCaT cells under the same experimental conditions (Fig. 4c). Co-treatments with WORT and CQ enhanced the pro-apoptotic effect of DOX and the accumulation of cleaved caspase-3 and PARP-1.

**Autophagy modulation in embryonic zebrafish cells**

Zebrafish embryos at 6 hpf were treated for 48 h with compounds at concentrations which modulated autophagy but did not affect embryo survival and development.

To confirm that autophagy modulators at selected concentrations interfered with the autophagy process, we assessed the cellular content of autophagy markers, LC3 and p62 in zebrafish embryos. Anti-LC3-labeled autophagosomes were visualized after 48 h treatment with WORT, CQ, AZD2014 or TMX and their combinations with CPt (Fig.5a). WORT treatment prevented the appearance of LC3 positive autophagic vesicles in the cytoplasm while CQ triggered their substantial accumulation. Autophagy induction with either AZD2014 or TMX resulted in increased LC3 puncta in the cytoplasm. Autophagy inhibition

with WORT and CQ also blocked p62 degradation leading to cytoplasmatic accumulation of this autophagy marker (Fig. 5b). The presence of CPt in co-treatments did not change the autophagy-modulating properties of the selected compounds.

**The effect of autophagy modulation on CPt-induced cell death in embryonic zebrafish cells**

To follow the changes in apoptosis patterns during zebrafish development in context of autophagy modulation, 6 hpf embryos were treated with WORT, CQ, AZD2014 or TMX and their combinations with CPt for 48 h. Application of autophagy modulators alone did not induce abnormal apoptosis patterns (Fig. 6a). After CPt treatment an increased amount of acridine orange-positive apoptotic cells was evident in the trunk, and especially in the tail region. Autophagy inhibition with WORT and CQ synergized with the pro-apoptotic effect of CPt, causing an additional increase of apoptotic cells in the trunk as well as the lens and retina region of the embryos. AZD2014 and TMX co-treatment prevented CPt-induced apoptosis significantly reducing the amount of acridine orange-positive cells in zebrafish embryos (Fig. 6a).

To assess the cellular distribution of apoptosis markers in embryonic zebrafish cells, embryos were labeled with antibodies for cleaved caspase-3 and PARP-1 (Fig. 6b). WORT and CQ co-treatment with CPt had a similar effect on the apoptotic markers' immunostaining as the application of CPt alone. AZD2014 and TMX co-treatment decreased cellular cleaved caspase 3 and PARP-1 content compared to a single CPt treatment, reducing cell death during embryogenesis in CPt-treated animals (Fig. 6b).

**Discussion**

Herein, we conducted a comparative study using three models - human cancer cells, human normal cells and zebrafish embryonic cells in order to elucidate how autophagy modulation affects the cell survival and sensitivity to anticancer drugs.

One of the initial steps in bioactive compounds testing includes evaluation of their biological effects on embryonic models. Testing of candidate cancer modulators on these models gives valuable insight on toxicity and tissue specificity as well as compound's growth arrest capacity of highly proliferative cells *in vivo*. Many cancer cells possess the ability to switch from a primarily oxidative metabolism to glycolysis even with abundant amounts of oxygen present (Smith and Sturmey 2013). A dramatic increase in aerobic glycolysis is also a main feature of the early embryo development. Aside from the similarity in metabolism

regulation, cancers and early embryos share a number of other analogies including invasive properties, constitutively active pathways, gene expression, and the capacity to undergo rapid proliferation (Smith and Sturmey 2013). Many of these features could be affected by autophagy, another fundamental process in both tumorigenicity and embryonic development.

Four autophagy-modulating compounds with different mechanisms of action were included in the study. The autophagy process in NCI-H460, HaCaT and embryonic zebrafish cells was altered after treatment with wortmannin, chloroquine, AZD2014 or tamoxifen. Wortmannin is a potent and specific phosphatidylinositol 3-kinase inhibitor with the capacity to suppress autophagosome formation which relies upon the activity of this kinase (Blommaart et al. 1997). Chloroquine, an antimalarial drug, is an indirect autophagy inhibitor which neutralizes lysosomal pH thereby inhibiting autophagosome clearance and disrupting the autophagic flux (Stern et al. 2012). AZD2014 is a small-molecule ATP competitive inhibitor of mTOR that directly inhibits both mTORC1 and mTORC2 complexes (Guichard et al. 2015). Tamoxifen is an antagonist of the estrogen receptor with an ability to indirectly induce autophagy by increasing the intracellular levels of ceramide, which then inhibits mTOR activation and stimulates the expression of Atg genes (Scarlatti et al. 2004).

Notably, autophagy modulators displayed varying growth arrest ability in cells depending on whether they directly acted on PI3kinase/Akt/mTOR pathway or indirectly modulated autophagy. Although NCI-H460 and HaCaT cells were most sensitive to direct inhibitors of the PI3kinase/Akt/mTOR pathway, WORT and AZD2014 were generally more active in all tested cell lines compared to indirect autophagy modulators. WORT and AZD2014 were over 1.5 fold and 3 fold more efficient, respectively, in NCI-H460 cells compared to HaCaT cells. The PI3kinase/Akt/mTOR pathway is constitutively activated in various types of cancer including non-small cell lung cancer cells and confers resistance to different cancer therapies (Assinder et al. 2009; Jeong et al. 2012). In NSCLC cells, the sensitivity to WORT was 30 fold higher in NCI-H460, and 3 fold higher in COR-L23 cells when compared to CQ. For comparison, MRC-5, a normal lung epithelial cell line, had nearly the same sensitivity for both autophagy inhibitors. Moreover, the efficiency of AZD2014 in NSCLC cells was notably higher than TMX when compared to compounds' activity in MRC-5 cell line. Accordingly, direct inhibition of the PI3kinase/Akt/mTOR pathway could trigger the cellular stress response more effectively in cancer cell lines suggesting that these inhibitors more selectively target cancer compared to normal cells.

Induction of apoptosis is a key mechanism behind the cytotoxicity of many chemotherapeutic agents. DOX is an anthracycline drug which, in addition to free radical

formation, also intercalates DNA and inhibits the action of topoisomerase II (Pommier et al. 2010). CPt is a platinum based chemotherapy drug used to treat various cancers. This alkylating agent is known to cause cross-linking and adduct formation by intercalating with DNA strands and promote generation of free radicals (Matsushima et al. 1998). Autophagy may play a pro-survival role and allow tumor growth under starvation or chemotherapy-induced cell death. Application of autophagy inhibitor 3-methyladenine as well as targeting Atg7 protein sensitized human colorectal cancer cells to 5-fluorouracil (Li et al. 2010). Autophagy inhibition also enhanced the therapeutic efficacy of CPt in esophageal squamous cell carcinoma cells (Liu et al. 2011). However, during increased or prolonged stress, autophagy can also lead cancer cells into apoptosis.

In our study, both autophagy inducers considerably diminished the growth inhibition effect that apoptotic agents DOX and CPt had on tested cell lines. AZD2014 and TMX demonstrated a strong antagonistic effect on either DOX or CPt activity. Interestingly, the observed antagonism according to CI values was more consistent in cancer cells, regardless of the DOX or CPt concentration. The strength of the antagonism in normal cells was largely dependent on the applied concentration of DOX and CPt. Moreover, the direct inhibition of mTOR by AZD2014 had a far more prominent antagonistic effect on DOX or CPt in cancer cells than indirect autophagy induction by TMX, particularly at higher DOX concentrations. Autophagy inhibitors, including CQ, have been previously reported to synergize with chemotherapeutic agents in killing cancer cells (Livesey et al. 2009). In our experiments, WORT, as a direct inhibitor of PI3 kinase was overall more efficient in synergizing with DOX in cancer cell lines compared to the indirect autophagic flux inhibition by CQ. As CI values indicate, synergistic effect of either autophagy inhibitor in combination with chemotherapeutics was more prominent in cancer cell lines, particularly in NCI-H460 and COR-L23 cells. NSCLC cell lines, NCI-H460 and COR-L23, both carry *KRAS* mutations (Looyenga et al. 2012; Chakrabarti 2015) unlike U87 glioblastoma cells which possess a wild type *KRAS* gene (Spangler et al. 2012). Ras-driven cancers are reported to depend on autophagy for metabolic support and this process is required to promote cell survival and rapid tumor growth (Avalos et al. 2014; Guo et al. 2011). Genetic or pharmacologic inhibition of autophagy leads to increased reactive oxygen species, triggers DNA damage, and promotes the accumulation of dysfunctional mitochondria in Ras-driven tumors (Avalos et al. 2014; Yang et al. 2011). Consequently, the synergistic effect of autophagy inhibitors with DOX or CPt in NSCLC cells could be the result of their *KRAS* mutational status. Moreover, in U87 cells CQ treatment exhibited synergism only at higher CPt doses while

synergistic effect was not observed with DOX. The synergism between autophagy inhibitors and chemotherapeutics in HaCaT and MRC-5 cells was not as pronounced, particularly in CPt co-treatments. These results imply that modulation of autophagy has a stronger impact on cancer cells compared to normal cells, what should be considered as an important characteristic for development of anticancer agents based on autophagy modulation.

Cell death analysis after co-treatments of autophagy modulators with DOX showed anti-apoptotic effect of autophagy induction in cancer cells. Autophagy inducers AZD2014 and TMX reduced the percentage of late apoptotic and necrotic cancer cells observed when DOX was applied alone. Autophagy inhibitors WORT and CQ had the opposite effect on cell viability and significantly amplified the pro-apoptotic effect of DOX. Interestingly, CQ inhibition of autophagic flux through blockage of lysosomal fusion mainly induced apoptosis while WORT autophagy inhibition at the early stage promoted necrotic cell death in NCI-H460 cells. In other NSCLC cell line, COR-L23, CQ co-treatment with DOX also predominantly induced apoptosis while WORT co-treatment triggered both apoptotic and necrotic cell death. Similarly to the effect on cell growth, autophagy induction affected the activity of DOX much less prominently in normal cells compared to cancer cells. On contrary, autophagy inhibition in HaCaT and MRC-5 cells, particularly by CQ, had a more notable effect on DOX-induced apoptosis and necrosis than in NCI-H460 cells. However, this is likely due to considerably higher sensitivity of these cell lines to CQ. Moreover, chloroquine, which has been reported to promote Akt activation (Halaby et al. 2013; Spears et al. 2016), raised pAkt levels in both cell lines and induced a higher response in more sensitive HaCaT cells. WORT, AZD2014 and TMX, as direct or indirect inhibitors of PI3kinase/Akt/mTOR pathway components, have previously been reported to negatively affect Akt activation (Ng et al. 2001; Dietze et al. 2004; Yu et al. 2016), and in our experimental system they either decreased or unaffected pAkt levels in NCI-H460 and HaCaT cells, respectively.

There are various zebrafish mutants with abnormal cell death patterns that can be used to study apoptosis or as models for anti-apoptotic drug screening (Parng 2005; Furutani-Seiki et al. 1996). Treatment with different compounds can also alter these specific patterns of apoptosis. Various pro-apoptotic agents can increase cell death while anti-apoptotic drugs can reduce the number of apoptotic cells in developing zebrafish (Detrich et al. 2010). In *Danio rerio*, CPt has been previously shown to cause ototoxicity and hair cell loss in lateral line (Ou et al. 2007; Uribe et al. 2013). We observed an increased amount of apoptotic cells in the trunk and tail region of 48 hpf zebrafish embryos after CPt treatment. Autophagy induction

with AZD2014 and TMX prevented CPt-induced apoptosis in zebrafish embryos. Autophagy inhibitors WORT and CQ further enhanced cell death in CPt-treated animals, amplifying the amount of apoptotic cells in the trunk and eye region in 48 hfp embryos. Similarly to results obtained in human cell lines, these findings suggest that autophagy modulators, regardless of their mechanism of action, have the potential to interact with pro-apoptotic agents in an antagonistic or synergistic manner. During early zebrafish embryo development the PI3kinase/Akt/mTOR pathway is active and crucial for numerous processes including cell proliferation, migration and angiogenesis (Sasore and Kennedy 2014). Therefore, similarly to human cancer cell lines, autophagy induction by direct targeting of PI3kinase/Akt/mTOR pathway with AZD2014 considerably prevented chemotherapeutic-induced cell death in embryonic zebrafish cells, almost completely eliminating the appearance of dead cells within the tail region.

Activated caspases, key players in apoptosis, cleave various proteins ultimately leading to loss of cell function and death. Caspase-3 is one of the main and most widespread effectors of this process (Li and Yuan 2008). The cleavage of PARP-1, another important component, promotes apoptosis by preventing DNA repair-induced survival (D'Amours et al. 2001) and this protein was also shown to be involved in the release of apoptosis-inducing factor from mitochondria in caspase-independent apoptosis (Yu et al. 2002).

DOX and CPt concentrations used in our experimental setup predominantly triggered apoptosis in investigated models. Modulation of autophagy in human cancer and normal cell lines as well as zebrafish embryos displayed a major effect on the pro-apoptotic activity of the chemotherapeutic agents. AZD2014 combination with DOX significantly decreased cleaved caspase-3 and PARP-1 in NCI-H460 cells, or only cleaved caspase-3 levels in HaCaT. Autophagy induction by TMX significantly blocked the activation of caspase-3 and PARP-1 in both cell lines during the co-treatment with DOX. Autophagy inhibition by WORT and CQ additionally activated either one or both apoptotic markers which were triggered by the application of DOX. Zhang and coworkers showed that inhibition of autophagy promoted caspase-mediated apoptosis in tunicamycin treated HepG2 cells as the activity of caspase-3, 7, 8, 9 and PARP-1 cleavage noticeably increased (Zhang et al. 2014). This finding is consistent with our observations that inhibition of autophagosome formation or autophagic flux triggered the cleavage of caspase-3 or PARP-1. Similar results were also observed in embryonic zebrafish cells. Modulation of the autophagy process in CPt-treated animals interfered with the cellular content of apoptotic markers. Co-treatment with

AZD2014 and TMX decreased caspase 3 and PARP-1 activation triggered by CPt in zebrafish embryos.

## Conclusion

In conclusion, our results stress the importance of testing autophagy inducing/inhibiting activity of new anticancer agents. Namely, in cancer treatment, autophagy may either enable cell survival or lead to cell death. Standard protocols for the investigation of new compounds include cell death induction testing. However, without an insight in autophagy properties, it is difficult to conclude whether a new anticancer agent could affect normal cells or lead to the development of resistance. In addition, the similarities that autophagy modulation shows in cancer and embryonic models confirm the role of this process in physiological development and tumorigenesis which are both dependent on cell growth and the level of differentiation. Therefore, the comparative approach presented in this study with cancer, normal and developmental cells could help in creating more rational anticancer therapeutic strategies.

## Compliance with ethical standards

All applicable international, national, and/or institutional guidelines for the care and use of animals were followed. All procedures performed in studies involving animals were in accordance with the ethical standards of the institution or practice at which the studies were conducted.

## Conflict of Interest

The authors declare no conflict of interest.

## Figure legends

**Fig.1** Sensitivity of NCI-H460 and HaCaT cells to pro-apoptotic agents after autophagy modulation (**a**) Cell growth inhibition in NCI-H460 and HaCaT cells assessed by MTT assay after 72 h treatment with DOX, CPt, WORT, CQ, AZD2014 or TMX. The average value ± SD was obtained from at least three independent experiments. (**b**) $IC_{50}$ values for DOX and CPt in single and co-treatments with WORT, CQ, AZD2014 or TMX in NCI-H460 and HaCaT cells. (**c**) Autophagy inducers antagonize while autophagy inhibitors synergize pro-apoptotic efficacy of DOX and CPt in NCI-H460 and HaCaT cells during co-treatments. CI

values which depict antagonistic effect ($log_{10}CI > 0$) or synergistic effect ($log_{10}CI < 0$) are represented on the Y-axis.

**Fig.2** Modulation of autophagy in NCI-H460 and HaCaT cells (**a**) Accumulation of autophagosomes in the cytoplasm after 72 h treatment with WORT, CQ, AZD2014 or TMX or their combination with DOX, was visualized after anti-LC3 antibody labeling. (**b**) Accumulation of autophagy marker p62 in the cytoplasm after 72 h treatment with WORT, CQ, AZD2014 or TMX or their combination with DOX, was visualized after anti-p62 antibody labeling. Nuclei were counterstained with Hoechst 33342. Scale bar = 50 μm.

**Fig.3** Autophagy induction by AZD2014 or TMX prevented DOX-induced cell death in NCI-H460 and HaCaT cells (**a**) Quantification and statistical analysis of flow-cytometric cell death measurements after 72 h treatment with WORT, CQ, AZD2014 or TMX or their combination with DOX. Statistical analysis was performed by two-way ANOVA test. Statistical significance between untreated and treated samples is presented as $p < 0.001$ (***). Statistical significance between DOX treatment and combination treatments is presented as $p < 0.001$ (###) and $p < 0.01$ (##). (**b**) Flow-cytometric profiles of cell death induction by WORT, CQ, AZD2014 or TMX in single and combination treatments with DOX for 72 h. The samples were analyzed for green fluorescence (Annexin V-FITC, FL1-H) and red fluorescence (PI, FL2-H).

**Fig.4** Autophagy induction decreased cleaved caspase-3 and PARP-1 levels in DOX-treated in NCI-H460 and HaCaT cells (**a**) Quantification and statistical analysis of cleaved caspase-3 (cCas-3) and cleaved PARP-1 (cPARP-1) content after 72 h treatment with WORT, CQ, AZD2014 or TMX or their combination with DOX. Statistical significance was determined by one-way ANOVA test and is presented as $p < 0.001$ (***), $p < 0.01$ (**) and $p < 0.05$ (*).Statistical significance between DOX treatment and combination treatments is presented as $p < 0.001$ (###) and $p < 0.01$ (##). (**b**) Flow-cytometric profiles of NCI-H460 and HaCaT cells treated for 72 h with WORT, CQ, AZD2014 or TMX or their combination with DOX after labeling with antibodies for apoptotic markers, cCas-3 and cPARP-1. The samples were analyzed in FL1-H channel for fluorescence intensity. (**c**) NCI-H460 and HaCaT cells were labeled for cCas-3 and cPARP-1 to visualize the cellular distribution of the apoptotic markers after 72 h treatment with WORT, CQ, AZD2014 or TMX or their combination with DOX. Nuclei were counterstained with Hoechst 33342. Scale bar = 50 μm.

**Fig.5** Modulation of autophagy in zebrafish embryos (**a**) Accumulation of autophagosomes in the cytoplasm after 48 h treatment with WORT, CQ, AZD2014 or TMX or their combination with CPt visualized with anti-LC3 antibody. (**b**) Accumulation of autophagy marker p62 in the cytoplasm after 48 h treatments with WORT, CQ, AZD2014 or TMX or their combination with CPt visualized with anti-p62 antibody. Images represent the tail region of the zebrafish embryo. Nuclei were counterstained with Hoechst 33342. Scale bar = 20 μm.

**Fig.6** Autophagy induction by AZD2014 or TMX prevented CPt-induced cell death of embryonic zebrafish cells (**a**) Live zebrafish embryos were stained with acridine orange after 48 h treatment with WORT, CQ, AZD2014 or TMX or their combination with CPt. After WORT/CPt and CQ/CPt co-treatments, acridine orange-positive apoptotic cells were found over the whole embryo and most abundantly within the head and the tail region. Insets on the right represent magnified head region of the zebrafish embryo. Scale bar = 250 μm. (**b**) Zebrafish embryos were labeled with anti-cleaved caspase 3 (cCas-3) and anti-cleaved PARP-1 (cPARP-1) antibodies to visualize the cellular distribution of the apoptotic markers after 48 h treatment with WORT, CQ, AZD2014 or TMX or their combination with CPt. Images represent the tail region of the zebrafish embryo. Nuclei were counterstained with Hoechst 33342. Scale bar = 20 μm.

**References**


Aburto MR, Hurle JM, Varela-Nieto I, Magarinos M (2012) Autophagy during vertebrate development. Cells 1 (3):428-448. doi:cells1030428 [pii]
10.3390/cells1030428

Aredia F, Guaman Ortiz LM, Giansanti V, Scovassi AI (2012) Autophagy and cancer. Cells 1 (3):520-534. doi:cells1030520 [pii]
10.3390/cells1030520

Assinder SJ, Dong Q, Kovacevic Z, Richardson DR (2009) The TGF-beta, PI3K/Akt and PTEN pathways: established and proposed biochemical integration in prostate cancer. Biochem J 417 (2):411-421. doi:BJ20081610 [pii]
10.1042/BJ20081610 [doi]

Avalos Y, Canales J, Bravo-Sagua R, Criollo A, Lavandero S, Quest AF (2014) Tumor suppression and promotion by autophagy. BioMed research international 2014:603980. doi:10.1155/2014/603980

Blommaart EF, Krause U, Schellens JP, Vreeling-Sindelarova H, Meijer AJ (1997) The phosphatidylinositol 3-kinase inhibitors wortmannin and LY294002 inhibit autophagy in isolated rat hepatocytes. Eur J Biochem 243 (1-2):240-246

Brand M, Heisenberg CP, Warga RM, Pelegri F, Karlstrom RO, Beuchle D, Picker A, Jiang YJ, Furutani-Seiki M, van Eeden FJ, Granato M, Haffter P, Hammerschmidt M, Kane DA, Kelsh RN, Mullins MC, Odenthal J, Nusslein-Volhard C (1996) Mutations affecting development of the midline and general body shape during zebrafish embryogenesis. Development 123:129-142

Chakrabarti G (2015) Mutant KRAS associated malic enzyme 1 expression is a predictive marker for radiation therapy response in non-small cell lung cancer. Radiation oncology 10:145. doi:10.1186/s13014-015-0457-x

Chou TC, Talalay P (1984) Quantitative analysis of dose-effect relationships: the combined effects of multiple drugs or enzyme inhibitors. Adv Enzyme Regul 22:27-55

Cole LK, Ross LS (2001) Apoptosis in the developing zebrafish embryo. Dev Biol 240 (1):123-142. doi:10.1006/dbio.2001.0432

S0012-1606(01)90432-4 [pii]

D'Amours D, Sallmann FR, Dixit VM, Poirier GG (2001) Gain-of-function of poly(ADP-ribose) polymerase-1 upon cleavage by apoptotic proteases: implications for apoptosis. J Cell Sci 114 (Pt 20):3771-3778

Detrich HW, 3rd, Westerfield M, Zon LI (2010) The zebrafish: cellular and developmental biology, part A. Preface. Methods Cell Biol 100:xiii. doi:B978-0-12-384892-5.00018-9 [pii]

10.1016/B978-0-12-384892-5.00018-9

Dietze EC, Troch MM, Bean GR, Heffner JB, Bowie ML, Rosenberg P, Ratliff B, Seewaldt VL (2004) Tamoxifen and tamoxifen ethyl bromide induce apoptosis in acutely damaged mammary epithelial cells through modulation of AKT activity. Oncogene 23 (21):3851-3862. doi:10.1038/sj.onc.1207480

Eskelinen EL, Saftig P (2009) Autophagy: a lysosomal degradation pathway with a central role in health and disease. Biochim Biophys Acta 1793 (4):664-673. doi:S0167-4889(08)00263-2 [pii]

10.1016/j.bbamcr.2008.07.014

Fimia GM, Piacentini M (2010) Regulation of autophagy in mammals and its interplay with apoptosis. Cell Mol Life Sci 67 (10):1581-1588. doi:10.1007/s00018-010-0284-z

Furutani-Seiki M, Jiang YJ, Brand M, Heisenberg CP, Houart C, Beuchle D, van Eeden FJ, Granato M, Haffter P, Hammerschmidt M, Kane DA, Kelsh RN, Mullins MC, Odenthal J, Nusslein-Volhard C (1996) Neural degeneration mutants in the zebrafish, Danio rerio. Development 123:229-239

Guichard SM, Curwen J, Bihani T, D'Cruz CM, Yates JW, Grondine M, Howard Z, Davies BR, Bigley G, Klinowska T, Pike KG, Pass M, Chresta CM, Polanska UM, McEwen R, Delpuech O, Green S, Cosulich SC (2015) AZD2014, an Inhibitor of mTORC1 and mTORC2, Is Highly Effective in ER+ Breast Cancer When Administered Using Intermittent or Continuous Schedules. Mol Cancer Ther 14 (11):2508-2518. doi:1535-7163.MCT-15-0365 [pii]

10.1158/1535-7163.MCT-15-0365

Guo JY, Chen HY, Mathew R, Fan J, Strohecker AM, Karsli-Uzunbas G, Kamphorst JJ, Chen G, Lemons JM, Karantza V, Coller HA, Dipaola RS, Gelinas C, Rabinowitz JD, White E (2011) Activated Ras requires autophagy to maintain oxidative metabolism and tumorigenesis. Genes Dev 25 (5):460-470. doi:10.1101/gad.2016311

Halaby MJ, Kastein BK, Yang DQ (2013) Chloroquine stimulates glucose uptake and glycogen synthase in muscle cells through activation of Akt. Biochem Biophys Res Commun 435 (4):708-713. doi:10.1016/j.bbrc.2013.05.047

Hippert MM, O'Toole PS, Thorburn A (2006) Autophagy in cancer: good, bad, or both? Cancer Res 66 (19):9349-9351. doi:66/19/9349 [pii]

10.1158/0008-5472.CAN-06-1597

Inohara N, Nunez G (2000) Genes with homology to mammalian apoptosis regulators identified in zebrafish. Cell Death Differ 7 (5):509-510. doi:10.1038/sj.cdd.4400679

Janji B, Viry E, Baginska J, Van Moer K, Berchem G (2013) Role of Autophagy in Cancer and Tumor Progression. In: Bailly Y (ed) Autophagy - A Double-Edged Sword - Cell Survival or Death? InTech. doi:10.5772/55388

Jeong EH, Choi HS, Lee TG, Kim HR, Kim CH (2012) Dual Inhibition of PI3K/Akt/mTOR Pathway and Role of Autophagy in Non-Small Cell Lung Cancer Cells. Tuberc Respir Dis (Seoul) 72 (4):343-351

Lee E, Koo Y, Ng A, Wei Y, Luby-Phelps K, Juraszek A, Xavier RJ, Cleaver O, Levine B, Amatruda JF (2014) Autophagy is essential for cardiac morphogenesis during vertebrate development. Autophagy 10 (4):572-587. doi:27649 [pii]

10.4161/auto.27649

Li J, Hou N, Faried A, Tsutsumi S, Kuwano H (2010) Inhibition of autophagy augments 5-fluorouracil chemotherapy in human colon cancer in vitro and in vivo model. Eur J Cancer 46 (10):1900-1909. doi:S0959-8049(10)00148-6 [pii]

10.1016/j.ejca.2010.02.021

Li J, Yuan J (2008) Caspases in apoptosis and beyond. Oncogene 27 (48):6194-6206. doi:onc2008297 [pii]

10.1038/onc.2008.297

Liu D, Yang Y, Liu Q, Wang J (2011) Inhibition of autophagy by 3-MA potentiates cisplatin-induced apoptosis in esophageal squamous cell carcinoma cells. Med Oncol 28 (1):105-111. doi:10.1007/s12032-009-9397-3

Livesey KM, Tang D, Zeh HJ, Lotze MT (2009) Autophagy inhibition in combination cancer treatment. Curr Opin Investig Drugs 10 (12):1269-1279

Looyenga BD, Hutchings D, Cherni I, Kingsley C, Weiss GJ, Mackeigan JP (2012) STAT3 is activated by JAK2 independent of key oncogenic driver mutations in non-small cell lung carcinoma. PLoS One 7 (2):e30820. doi:10.1371/journal.pone.0030820

Martinet W, Agostinis P, Vanhoecke B, Dewaele M, De Meyer GR (2009) Autophagy in disease: a double-edged sword with therapeutic potential. Clin Sci (Lond) 116 (9):697-712. doi:CS20080508 [pii]

10.1042/CS20080508

Mathew R, Karantza-Wadsworth V, White E (2007) Role of autophagy in cancer. Nat Rev Cancer 7 (12):961-967. doi:nrc2254 [pii]

10.1038/nrc2254
Matsushima H, Yonemura K, Ohishi K, Hishida A (1998) The role of oxygen free radicals in cisplatin-induced acute renal failure in rats. J Lab Clin Med 131 (6):518-526. doi:S0022-2143(98)90060-9 [pii]
Meijer AJ, Codogno P (2004) Regulation and role of autophagy in mammalian cells. Int J Biochem Cell Biol 36 (12):2445-2462. doi:10.1016/j.biocel.2004.02.002
S1357272504000536 [pii]
Mizushima N, Yoshimori T, Levine B (2010) Methods in mammalian autophagy research. Cell 140 (3):313-326. doi:S0092-8674(10)00063-2 [pii]
10.1016/j.cell.2010.01.028
Ng SS, Tsao MS, Nicklee T, Hedley DW (2001) Wortmannin inhibits pkb/akt phosphorylation and promotes gemcitabine antitumor activity in orthotopic human pancreatic cancer xenografts in immunodeficient mice. Clinical cancer research : an official journal of the American Association for Cancer Research 7 (10):3269-3275
Ou HC, Raible DW, Rubel EW (2007) Cisplatin-induced hair cell loss in zebrafish (Danio rerio) lateral line. Hear Res 233 (1-2):46-53. doi:S0378-5955(07)00178-5 [pii]
10.1016/j.heares.2007.07.003
Parng C (2005) In vivo zebrafish assays for toxicity testing. Curr Opin Drug Discov Devel 8 (1):100-106
Pommier Y, Leo E, Zhang H, Marchand C (2010) DNA topoisomerases and their poisoning by anticancer and antibacterial drugs. Chem Biol 17 (5):421-433. doi:S1074-5521(10)00161-4 [pii]
10.1016/j.chembiol.2010.04.012
Sasore T, Kennedy B (2014) Deciphering combinations of PI3K/AKT/mTOR pathway drugs augmenting anti-angiogenic efficacy in vivo. PLoS One 9 (8):e105280. doi:10.1371/journal.pone.0105280 [doi]
PONE-D-14-06403 [pii]
Scarlatti F, Bauvy C, Ventruti A, Sala G, Cluzeaud F, Vandewalle A, Ghidoni R, Codogno P (2004) Ceramide-mediated macroautophagy involves inhibition of protein kinase B and up-regulation of beclin 1. J Biol Chem 279 (18):18384-18391. doi:10.1074/jbc.M313561200
M313561200 [pii]
Smith DG, Sturmey RG (2013) Parallels between embryo and cancer cell metabolism. Biochem Soc Trans 41 (2):664-669. doi:BST20120352 [pii]
10.1042/BST20120352 [doi]
Spangler JB, Manzari MT, Rosalia EK, Chen TF, Wittrup KD (2012) Triepitopic antibody fusions inhibit cetuximab-resistant BRAF and KRAS mutant tumors via EGFR signal repression. J Mol Biol 422 (4):532-544. doi:10.1016/j.jmb.2012.06.014
Spears LD, Tran AV, Qin CY, Hobbs SB, Burns CA, Royer NK, Zhang Z, Ralston L, Fisher JS (2016) Chloroquine increases phosphorylation of AMPK and Akt in myotubes. Heliyon 2 (3):e00083. doi:10.1016/j.heliyon.2016.e00083

Stern ST, Adiseshaiah PP, Crist RM (2012) Autophagy and lysosomal dysfunction as emerging mechanisms of nanomaterial toxicity. Part Fibre Toxicol 9:20. doi:1743-8977-9-20 [pii]
10.1186/1743-8977-9-20
Tanida I, Minematsu-Ikeguchi N, Ueno T, Kominami E (2005) Lysosomal turnover, but not a cellular level, of endogenous LC3 is a marker for autophagy. Autophagy 1 (2):84-91. doi:1697 [pii]
Thompson CB (1995) Apoptosis in the pathogenesis and treatment of disease. Science 267 (5203):1456-1462
Uribe PM, Mueller MA, Gleichman JS, Kramer MD, Wang Q, Sibrian-Vazquez M, Strongin RM, Steyger PS, Cotanche DA, Matsui JI (2013) Dimethyl sulfoxide (DMSO) exacerbates cisplatin-induced sensory hair cell death in zebrafish (Danio rerio). PLoS One 8 (2):e55359. doi:10.1371/journal.pone.0055359
PONE-D-12-25684 [pii]
Varga M, Sass M, Papp D, Takacs-Vellai K, Kobolak J, Dinnyes A, Klionsky DJ, Vellai T (2014) Autophagy is required for zebrafish caudal fin regeneration. Cell Death Differ 21 (4):547-556. doi:cdd2013175 [pii]
10.1038/cdd.2013.175
Westerfield M (2000) The zebrafish book. A guide for the laboratory use of zebrafish (Danio rerio). Eugene: University of Oregon Press,
Yang S, Wang X, Contino G, Liesa M, Sahin E, Ying H, Bause A, Li Y, Stommel JM, Dell'antonio G, Mautner J, Tonon G, Haigis M, Shirihai OS, Doglioni C, Bardeesy N, Kimmelman AC (2011) Pancreatic cancers require autophagy for tumor growth. Genes Dev 25 (7):717-729. doi:10.1101/gad.2016111
Yu CC, Huang HB, Hung SK, Liao HF, Lee CC, Lin HY, Li SC, Ho HC, Hung CL, Su YC (2016) AZD2014 Radiosensitizes Oral Squamous Cell Carcinoma by Inhibiting AKT/mTOR Axis and Inducing G1/G2/M Cell Cycle Arrest. PLoS One 11 (3):e0151942. doi:10.1371/journal.pone.0151942
Yu SW, Wang H, Poitras MF, Coombs C, Bowers WJ, Federoff HJ, Poirier GG, Dawson TM, Dawson VL (2002) Mediation of poly(ADP-ribose) polymerase-1-dependent cell death by apoptosis-inducing factor. Science 297 (5579):259-263. doi:10.1126/science.1072221
297/5579/259 [pii]
Zhang S, Wang C, Tang S, Deng S, Zhou Y, Dai C, Yang X, Xiao X (2014) Inhibition of autophagy promotes caspase-mediated apoptosis by tunicamycin in HepG2 cells. Toxicol Mech Methods 24 (9):654-665. doi:10.3109/15376516.2014.956915

**Table 1**. The range of concentrations for autophagy modulating agents and anticancer drugs applied on NCI-H460, COR-L23, U87, HaCaT and MRC-5 cells

| | **Drug concentrations** | | | | | |
|---|---|---|---|---|---|---|
| | WORT | CQ | AZD2014 | TMX | DOX | CPt |
| **NCI-H460** | 0.1 - 10 μM | 25 - 200 μM | 10 - 250 nM | 5 - 25 μM | 2.5 - 50 nM | 0.25 - 5 μM |
| **COR-L23** | 0.5 - 20 μM | 10 - 200 μM | 10 - 250 nM | 5 - 25 μM | 10 - 100 nM | 0.25 - 5 μM |
| **U87** | 0.5 - 20 μM | 10 - 150 μM | 10 - 250 nM | 1 - 25 μM | 10 - 100 nM | 0.25 - 5 μM |
| **HaCaT** | 0.5 - 20 μM | 5 - 100 μM | 10 - 250 nM | 5 - 25 μM | 10 - 100 nM | 1 - 10 μM |
| **MRC-5** | 0.5 - 20 μM | 10 - 200 μM | 50 - 1000 nM | 5 - 25 μM | 10 - 100 nM | 1 - 10 μM |

**Table 2**. The $IC_{50}$ values for autophagy modulators, classic anticancer drugs and their combinations in NCI-H460, COR-L23, U87, HaCaT and MRC-5 cells

| | **$IC_{50}$ (μM)** | | | | |
|---|---|---|---|---|---|
| | **NCI-H460** | **COR-L23** | **U87** | **HaCaT** | **MRC-5** |
| WORT | 4.7 | 13.3 | 14.7 | 7.3 | 16.7 |
| CQ | 137.5 | 40 | 36.4 | 15 | 18.3 |
| AZD2014 | 0.046 | 0.237 | 0.25 | 0.136 | 0.449 |
| TMX | 13.9 | 12.5 | 5.6 | 14.2 | 6.7 |
| DOX | 0.041 | 0.078 | 0.083 | 0.029 | 0.079 |
| DOX (+ WORT) | 0.025 | 0.033 | 0.032 | 0.01 | 0.06 |
| DOX (+ CQ) | 0.029 | 0.065 | 0.087 | 0.008 | 0.026 |
| DOX (+ AZD2014) | 0.071 | 0.093 | 0.106 | 0.069 | 0.14 |
| DOX (+ TMX) | 0.1 | 0.105 | 0.142 | 0.087 | 0.167 |
| CPt | 4.3 | 1.5 | 2.7 | 2.9 | 3.4 |
| CPt (+ WORT) | 2.1 | 0.5 | 0.5 | 2.6 | 2.9 |
| CPt (+ CQ) | 1.9 | 0.6 | 2.9 | 1.8 | 0.3 |
| CPt (+ AZD2014) | 5 | 4.8 | 2.9 | 15.8 | 4.4 |
| CPt (+ TMX) | 37.5 | 2.4 | 3.3 | 14.4 | 5.1 |

**Figure 1**

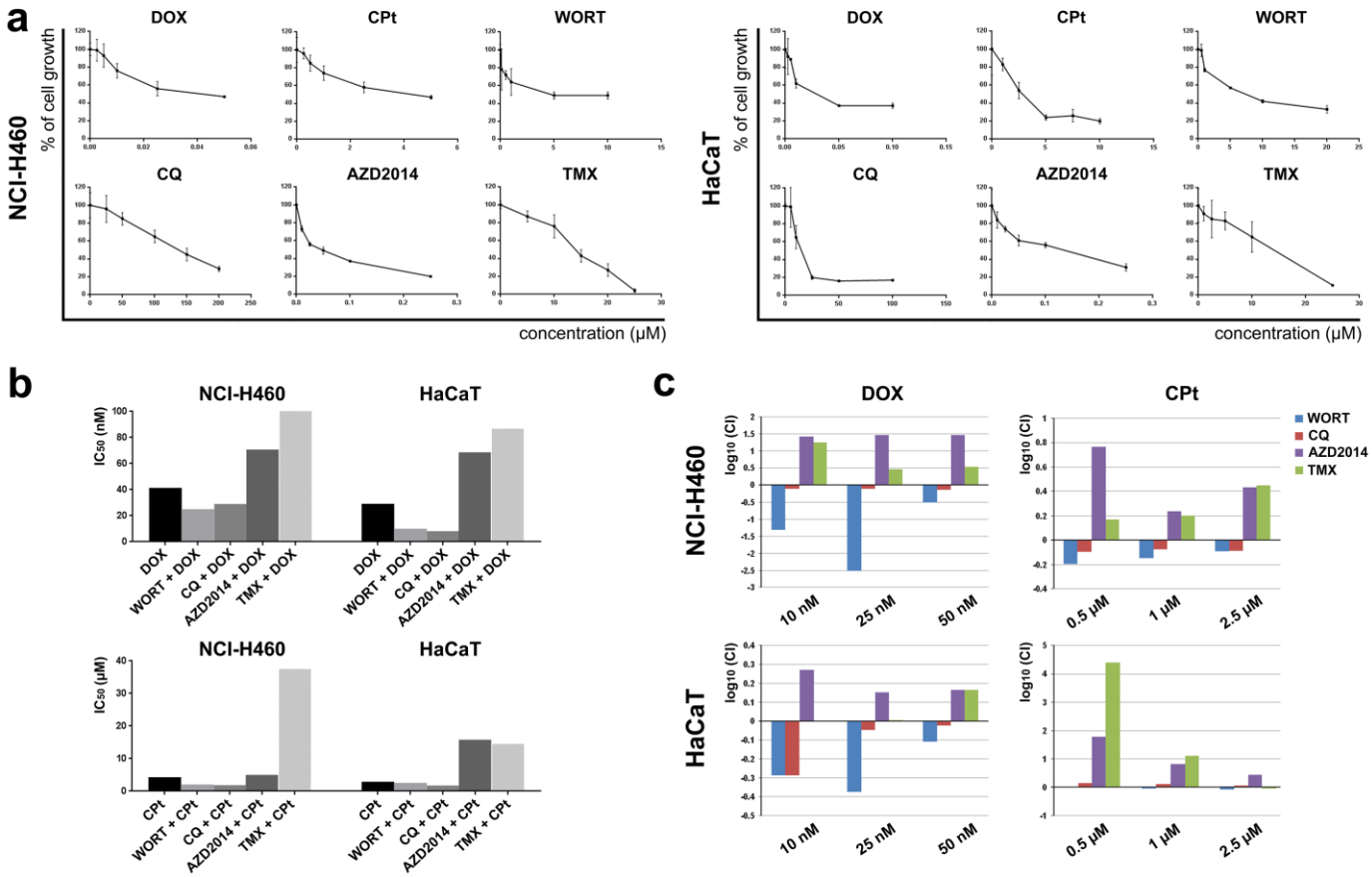
a
NCI-H460
HaCaT
% of cell growth
DOX
CPt
WORT
CQ
AZD2014
TMX
concentration (μM)
b
NCI-H460
HaCaT
IC50 (nM)
IC50 (μM)
DOX
WORT + DOX
CQ + DOX
AZD2014 + DOX
TMX + DOX
CPt
WORT + CPt
CQ + CPt
AZD2014 + CPt
TMX + CPt
c
DOX
CPt
log10 (CI)
10 nM
25 nM
50 nM
0.5 μM
1 μM
2.5 μM
WORT
CQ
AZD2014
TMX

**Figure 2**

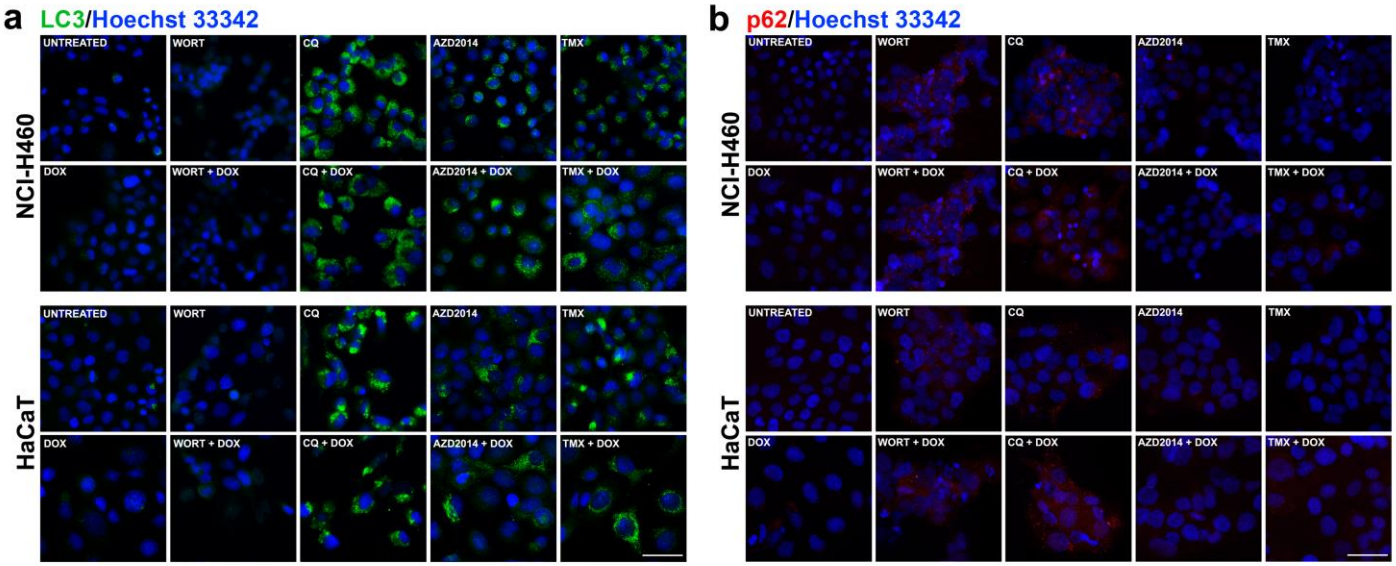
a
LC3/Hoechst 33342
b
p62/Hoechst 33342
NCI-H460
HaCaT
UNTREATED
WORT
CQ
AZD2014
TMX
DOX
WORT + DOX
CQ + DOX
AZD2014 + DOX
TMX + DOX

**Figure 3**

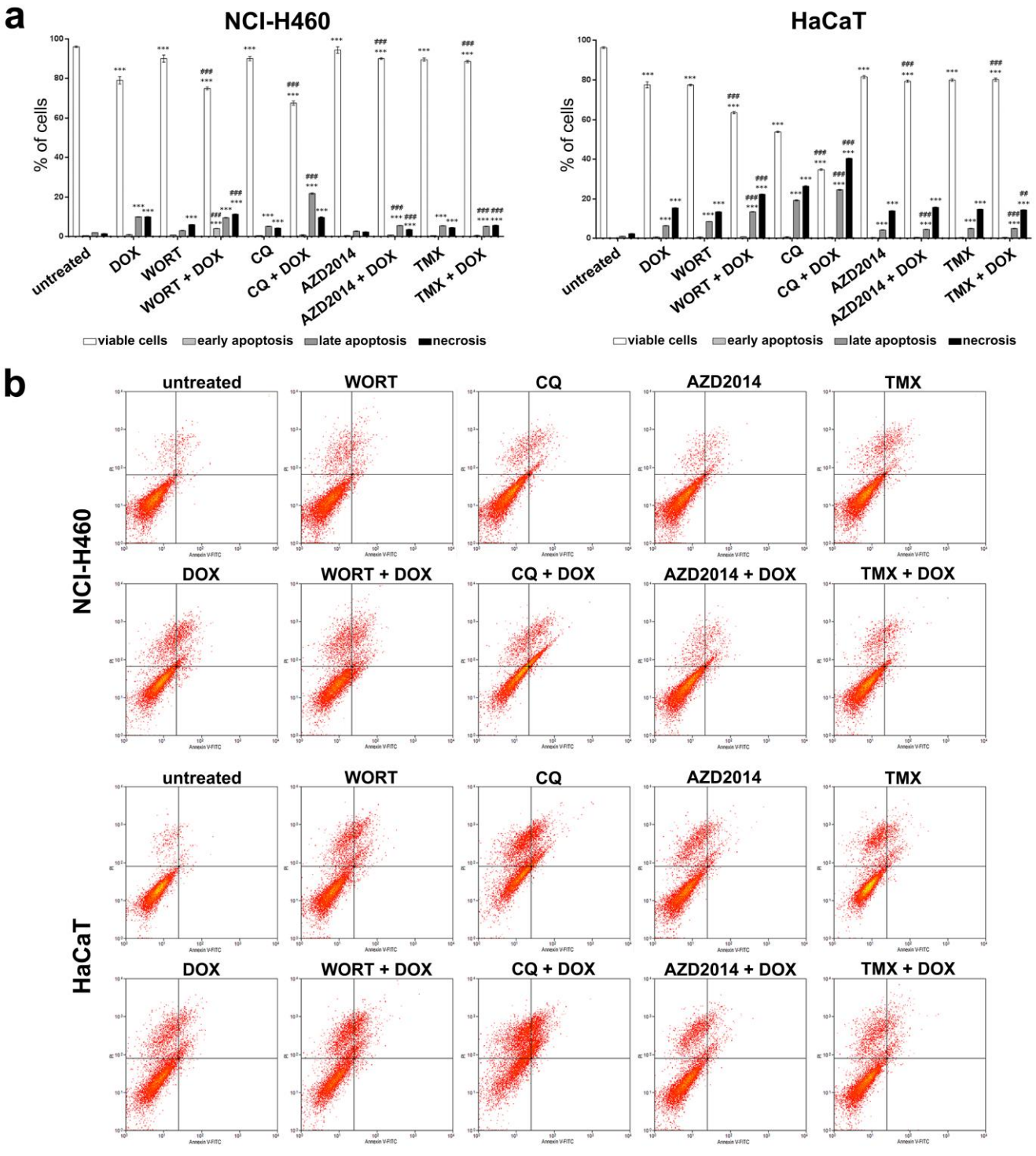
a
NCI-H460
HaCaT
% of cells
untreated
DOX
WORT
WORT + DOX
CQ
CQ + DOX
AZD2014
AZD2014 + DOX
TMX
TMX + DOX
viable cells
early apoptosis
late apoptosis
necrosis
b
NCI-H460
HaCaT
untreated
WORT
CQ
AZD2014
TMX
DOX
WORT + DOX
CQ + DOX
AZD2014 + DOX
TMX + DOX
Annexin V-FITC

**Figure 4**

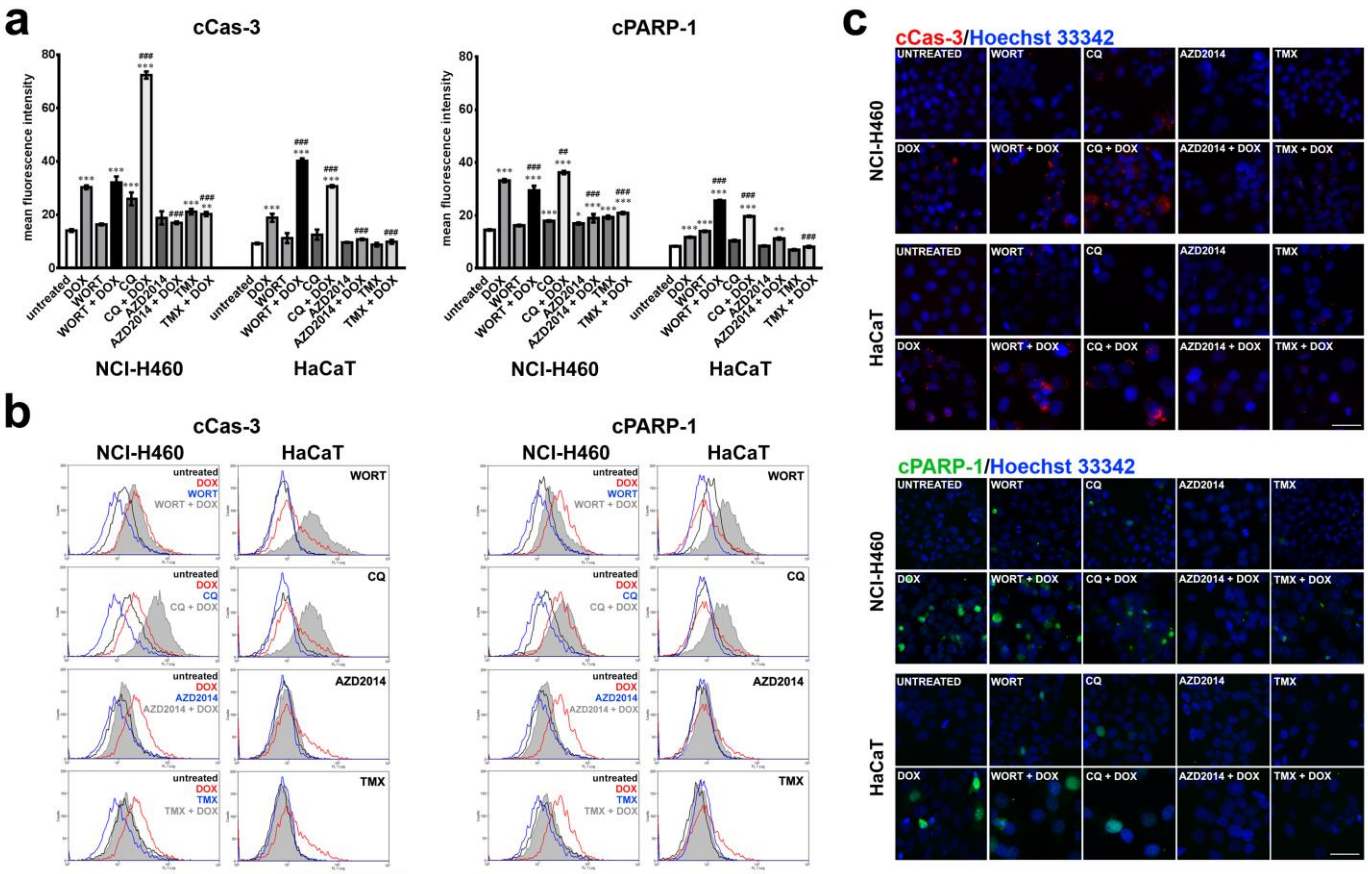
a
cCas-3
cPARP-1
mean fluorescence intensity
NCI-H460
HaCaT
untreated
DOX
WORT
WORT + DOX
CQ
CQ + DOX
AZD2014
AZD2014 + DOX
TMX
TMX + DOX
b
cCas-3
cPARP-1
NCI-H460
HaCaT
WORT
CQ
AZD2014
TMX
c
cCas-3/Hoechst 33342
cPARP-1/Hoechst 33342
UNTREATED
WORT
CQ
AZD2014
TMX
DOX
WORT + DOX
CQ + DOX
AZD2014 + DOX
TMX + DOX
NCI-H460
HaCaT

**Figure 5**

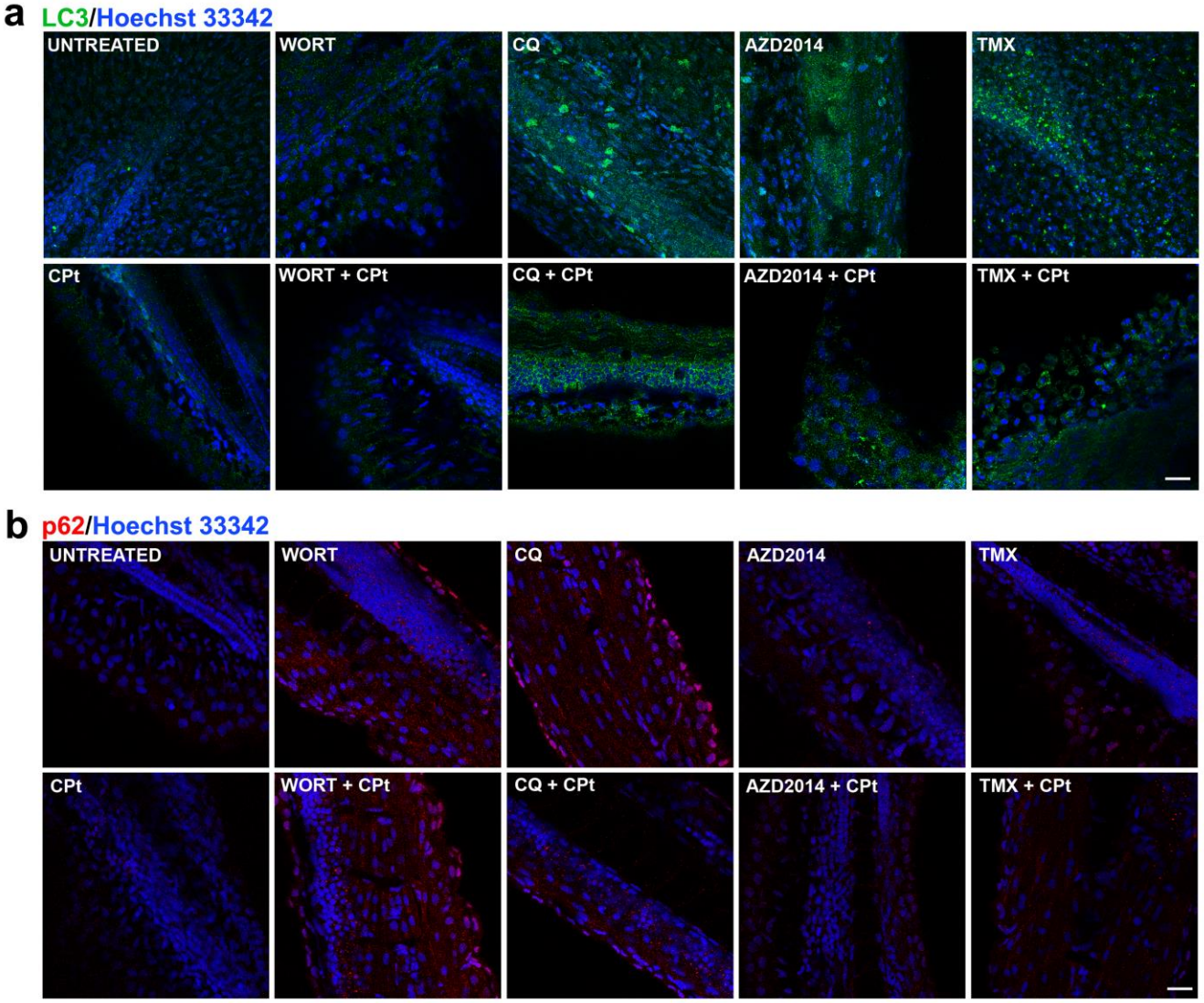
a
LC3/Hoechst 33342
UNTREATED
WORT
CQ
AZD2014
TMX
CPt
WORT + CPt
CQ + CPt
AZD2014 + CPt
TMX + CPt
b
p62/Hoechst 33342
UNTREATED
WORT
CQ
AZD2014
TMX
CPt
WORT + CPt
CQ + CPt
AZD2014 + CPt
TMX + CPt

**Figure 6**

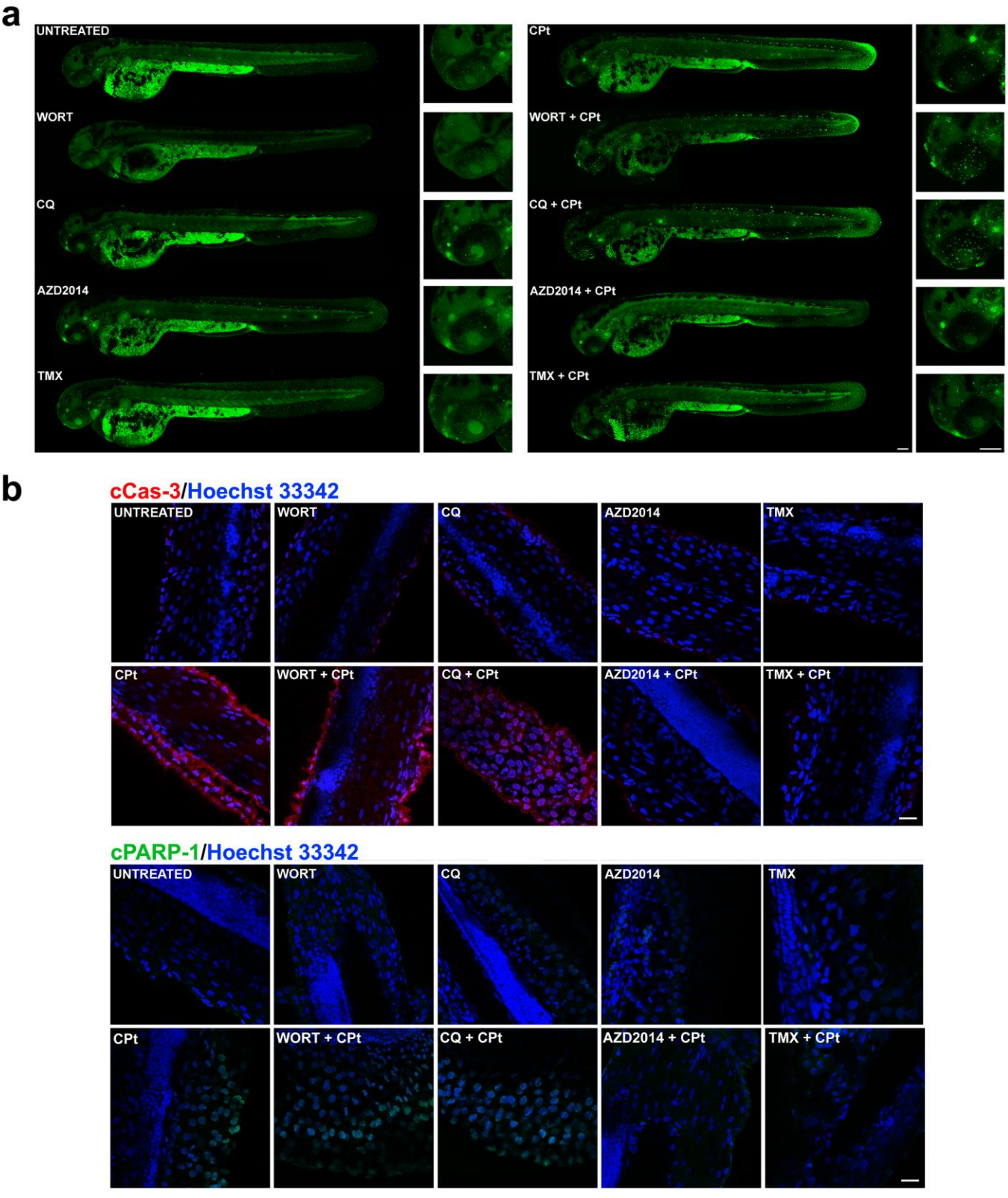
a
UNTREATED
WORT
CQ
AZD2014
TMX
CPt
WORT + CPt
CQ + CPt
AZD2014 + CPt
TMX + CPt
b
cCas-3/Hoechst 33342
UNTREATED
WORT
CQ
AZD2014
TMX
CPt
WORT + CPt
CQ + CPt
AZD2014 + CPt
TMX + CPt
cPARP-1/Hoechst 33342
UNTREATED
WORT
CQ
AZD2014
TMX
CPt
WORT + CPt
CQ + CPt
AZD2014 + CPt
TMX + CPt